

Preliminary Evaluation of a Solar-Powered Wristband for Continuous Multi-Modal Electrochemical Monitoring

Tanner Songkakul¹, Student Member, IEEE, Kaila Peterson¹, Student Member, IEEE,
Michael Daniele^{1,2}, Senior Member, IEEE, Alper Bozkurt¹, Senior Member, IEEE

Abstract—Continuous, non-invasive wearable measurement of metabolic biomarkers could provide vital insight into patient condition for personalized health and wellness monitoring. We present our efforts towards developing a wearable solar-powered electrochemical platform for multi-modal sweat based metabolic monitoring. This wrist-worn wearable system consists of a flexible photovoltaic cell connected to a circuit board containing ultra low power circuitry for sensor data collection, energy harvesting, and wireless data transmission, all integrated into an elastic fabric wristband. The system continuously samples amperometric, potentiometric, temperature, and motion data and wirelessly transmits these to a data aggregator. The full wearable system is 7.5 cm long and 5 cm in diameter, weighs 22 grams, and can run directly from harvested light energy. Relatively low levels of light such as residential lighting (~200 lux) are sufficient for continuous operation of the system. Excess harvested energy is stored in a small 37 mWh lithium polymer battery. The battery can be charged in ~14 minutes under full sunlight and can power the system for ~8 days when fully charged. The system has an average power consumption of 176 μ W. The solar-harvesting performance of the system was characterized in a variety of lighting conditions, and the amperometric and potentiometric electrochemical capabilities of the system were validated *in vitro*.

Clinical relevance—The presented solar-powered wearable system enables continuous wireless multi-modal electrochemical monitoring for uninterrupted sensing of metabolic biomarkers in sweat while harvesting energy from indoor lighting or sunlight.

I. BACKGROUND

Wearable health and wellness monitoring systems (wearables) have been demonstrated to provide physiologically relevant and actionable data in remote monitoring, fitness sensing, and personalized healthcare [1]-[3]. While wearable consumer products have the benefit of being non-invasive and easy to use, there is still a need to measure clinically-validated metabolic biomarkers such as glucose, lactate, and pH to give deeper insight into the users' health status [4][5]. These key metabolic biomarkers can be measured in eccrine sweat, which originates from pores distributed across the skin and is easily and continuously accessible [6]. In recent years,

*The authors acknowledge support from the National Science Foundation (NSF) through grant EEC-1160483 provided to the Center for Advanced Self-Powered Systems of Integrated Sensors and Technologies (ASSIST).

¹T. Songkakul, K. Peterson, M. Daniele, and A. Bozkurt are with the Department of Electrical Engineering, North Carolina State University, Raleigh, NC 27695, USA, corresponding e-mail: aybozkur@ncsu.edu.

²M. Daniele is with the Joint Department of Biomedical Engineering, North Carolina State University, Raleigh, NC 27606 USA, and University of North Carolina, Chapel Hill, NC 27514 USA.

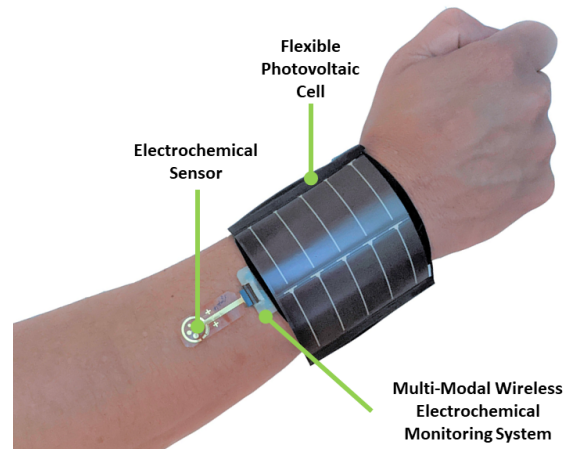


Fig. 1. The presented system consisting of a custom miniaturized wireless multi-modal electrochemical monitoring system which harvests light energy from a flexible photovoltaic cell integrated into a flexible wristband.

wearable sensors and systems measuring these biomarkers in eccrine sweat have been explored in a variety of form factors [7]-[13].

The continuous monitoring of such metabolic biomarkers can provide a deeper perspective on the correlation between their acute changes and patients' health outcomes. Continuous glucose monitors (CGMs) are a prime example of the potential benefits of such a continuous monitoring paradigm. Despite requiring transdermal access or implant, modern CGMs provide patients and caregivers with real-time feedback, allowing diabetic patients to improve their overall glucose control while reducing the likelihood of adverse events [14]. Extending and augmenting continuous biochemical monitoring with other metrics while removing the need to cross the skin barrier by continuously monitoring eccrine sweat could enable new use cases, especially when paired with a data aggregation device for data display and feedback or transmission to a cloud server for further analysis.

To achieve long term and continuous monitoring, state-of-the-art biochemical wearables rely on large lithium polymer (LiPo) batteries, in particular due to the higher power requirements of wireless data transmission. These batteries are bulky and require periodic recharging, forming a barrier for long term adoption and compliance [15]. Recent advances in energy harvesting and storage technologies have resulted in the development of wearable electrochemical systems which can be powered by solar, radio frequency, piezoelectric, biochemical or thermoelectric sources as an alternative or

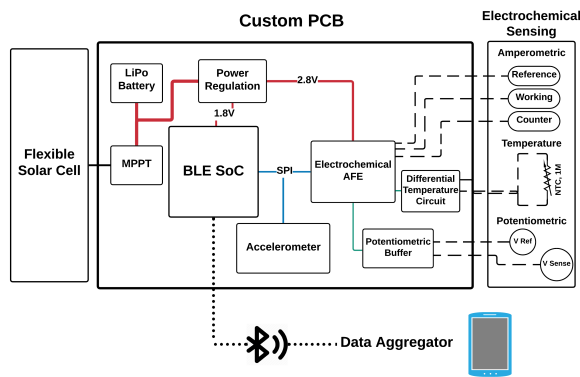


Fig. 2. System-level block diagram of the solar-powered electrochemical monitoring system.

augmentation to battery power [16]-[21]. However, these devices still fall short in offering continuous monitoring, ability to transmit data to a data aggregator, and multi-modal data acquisition to correlate biochemical data with other relevant health metrics.

In this work, we present our initial characterization of a solar-powered wristband for continuous multi-modal metabolic monitoring and wireless data transmission (Fig. 1). This system utilizes commercial-off-the-shelf (COTS) components to interface with custom electrochemical sensors, and includes an amperometric channel for analyte monitoring, a potentiometric channel for pH monitoring, a temperature interface for skin-temperature sensing, and an accelerometer for motion sensing (Fig. 2). The system can perform both cyclic voltammetry (CV) and chronoamperometry (CA), and measured data is transmitted to a data aggregator over Bluetooth Low Energy (BLE). This system can run directly and solely from harvested light energy, and stores excess amounts of energy into a small LiPo battery to prevent interruption of monitoring in darker environments. The energy harvesting and electrochemical sensing capabilities of this system were validated *in vitro* in the scope of this paper.

II. MATERIALS AND METHODS

A. System Overview

We designed a custom printed circuit board (PCB) for energy harvesting, power management, data acquisition, data transmission, and physiological monitoring (Fig. 3). To facilitate future transition onto a flexible PCB substrate, we designed the circuit board with layout islands and flex points, and restricted component placement to a single side.

A System-on-Chip (SoC, CC2642 from Texas Instruments (TI)) manages sampling and BLE transmission. The electrochemical analog front end (AFE, AD5941 from Analog Devices, Inc (ADI)) integrates the circuitry required for 3-electrode amperometric measurement. The SoC sets the bias, gain, and sampling rate of the AFE so that the system can perform CV at varying sweep rates or CA at varying sampling rates and bias points. An 8-pin Flat Flex Connector

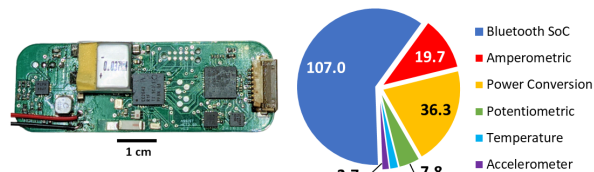


Fig. 3. (Left) The printed circuit board and 37 mWh LiPo battery. (Right) Power consumption breakdown by component subsystem in μW .

header (FH12-8S-1SH(55) from Molex) allows the device to interface to custom fabricated sensors.

The AFE also contains 4 analog to digital converter (ADC) channels, which we have utilized for pH and temperature measurements. Measurement of open-circuit potential (OCP) of a pH electrode is achieved through an op-amp buffer circuit (LPV542 from TI). Temperature measurement is achieved with a differential voltage Wheatstone bridge circuit to measure resistance change across a $1\text{M}\Omega$ negative temperature coefficient thermistor in response to changes in temperature. Interfacing the additional measurement channels to the AFE in this manner allows for increased power saving, as the SoC can spend more time in low-power sleep mode while the AFE samples the sensors. In CA mode, the AFE measures and stores 10 samples of amperometric, potentiometric, and temperature data at user configurable sampling rates of up to 10 Hz. The AFE, then, triggers an interrupt to the SoC, which reads the stored data and transmits it to a data aggregator via BLE. The system also contains a 3-axis accelerometer (ADXL362 from ADI) for aggregation of motion data for each sampling epoch.

Energy is harvested from a flexible photovoltaic (PV) cell (LL200-2.4-75 from PowerFilm) via a Maximum Power Point Tracking (MPPT) integrated boost regulator (bq25570 from TI). For this system, the MPPT is configured to set the load voltage at 77% of the open circuit voltage of the PV cells. The voltage generated is regulated to 1.8V for the SoC by a buck regulator built into the MPPT, and 2.8V for the rest of the system via a boost regulator (TPS62742 from TI). Excess power generated by the energy harvester is stored in a 37 mWh LiPo battery (PGEB201212 from Powerstream) to allow for uninterrupted monitoring in dim or no light conditions such as during sleep.

We integrated the PCB, battery, and PV cells with an elastic fabric sleeve to create a wrist-worn wearable system. To increase comfort for the wearer and protect the electronics from environmental exposure, we encapsulated the PCB and battery with flexible silicone (DragonSkin30 from Smooth-On) in a 3D printed mold. We developed a BLE user interface in Python for system control and data aggregation.

B. Energy Harvesting Characterization

To measure typical energy harvester output in various lighting conditions, we performed a proof-of-concept light harvesting characterization both indoors and outdoors. To measure average power from the energy harvester in each of these conditions, the system load was replaced by a known

load resistor. Average power generation was calculated by measuring average voltage from the light harvesting circuit across the load resistor for 10 minutes at a sampling rate of 1 Hz. Illuminance was recorded every 30 seconds using a handheld digital light meter (LX1330B from Dr.meter) and averaged. To measure battery charge time, the LiPo battery was discharged to 3.0V, then attached to the system and charged to 4.2V in full sunlight by the light harvesting circuitry on the PCB while the system was actively measuring data and transmitting over BLE.

C. In-Vitro Electrochemical Validation

CV measurements were performed using commercial screen-printed carbon electrodes (RRPE1001C from Pine Research) in a solution of 10 mM $K_3Fe(CN)_6$ and 1M KCL in 0.1 M phosphate buffered saline (PBS, pH=7.4, purchased from Sigma-Aldrich). We used a benchtop potentiostat (Reference 600+ from Gamry Instruments) to record CV measurements at sweep rates from 10 to 250 mV/s with scan limits from -0.6 to +0.6 V. We, then, performed CV measurements using the same carbon electrode and solution with the solar-powered electrochemical system at the same sweep rate and scan limit parameters.

To validate CA functionality, we performed CA measurements in various concentrations of glucose in 1M PBS using commercial blood glucose test strips (37350 Plus from AimStrip). We measured glucose concentrations from 1 mM to 100 mM at a bias of +0.5V with the benchtop potentiostat, then repeated these CA measurements at 1 Hz sampling rate using the solar-powered electrochemical system (n=3). Due to the microfluidic channel present on these test strips, a separate test strip was used for each measurement.

To validate potentiometric electrochemical sensing, a commercial pH electrode (pHE-11 from GeneMate) was connected to the potentiometric channel of the solar-powered electrochemical system. The pH electrodes were placed into buffer solutions between pH 4 and 10 purchased from Fisher Scientific, and the resulting OCP was measured by our system at a 1 Hz sampling frequency for 120 seconds. To reduce high electromagnetic interference (EMI) noise from the high-impedance pH electrode, an aluminum foil

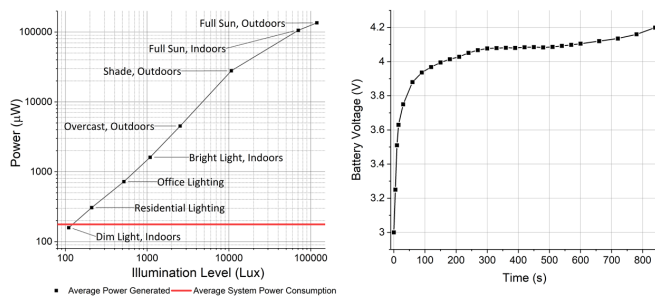


Fig. 4. (Left) Log-log comparison of average measured power generated by the energy-harvesting system at various representative lighting conditions versus average system power consumption at 10 s sampling period and BLE transmission at every 100 s. (Right) Battery charge in full sunlight during active measurement and transmission.

sheet was used to provide EMI shielding and the measured potentiometric data was smoothed with a 10 second moving average (MA) filter.

III. RESULTS AND DISCUSSION

A. Wearable System Integration

The encapsulated wireless electrochemical system has dimensions of 6 cm × 2.5 cm × 0.5 cm, and weighs 11 g. The integrated PV cells and elastic sleeve also weigh 11 g (total weight: 22 g). In an unexpanded state, the system is 7.5 cm tall and 5 cm in diameter, and can stretch to fit users with various body sizes.

B. System Power Consumption and Energy Harvesting

At a sampling period of 10 seconds, while transmitting data every 100 seconds, average total system power consumption was 176 μW , with majority of the power consumed by the SoC, power conversion efficiency loss, and amperometric measurement (Fig. 3). A fully charged 37 mWh battery provides 188 hours (7.8 days) of operation time at 90% discharge efficiency.

The light harvester generates an average of 135.4 mW in full sunlight (118,000 lux), which is sufficient to simultaneously power the device and charge the on-board battery from 3.0V to 4.2V in 14 minutes (Fig. 4). Residential indoor light levels (210 lux) generate an average of 306 μW , which is sufficient to power the system continuously due to the ultra-low power consumption of the electronic system (Fig. 4).

C. In-Vitro Electrochemical Validation

CV tests were performed using both the benchtop potentiostat and our solar-powered electrochemical sensing system at sweep rates between 10 mV/s and 250 mV/s in a $K_3Fe(CN)_6$ solution (n=1) (Fig. 5). The anodic and cathodic current peaks from both the solar-powered system and the benchtop potentiostat demonstrated the expected high linearity of current peaks as a function of the square root of the sweep rate ($R^2 \geq 0.9896$).

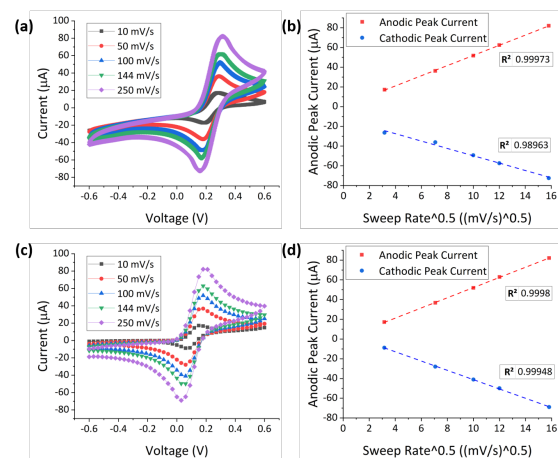


Fig. 5. CV at various sweep rates and square root of sweep rate versus peak anodic and cathodic currents for (a,b) the benchtop potentiostat and (c,d) the solar-powered electrochemical system.

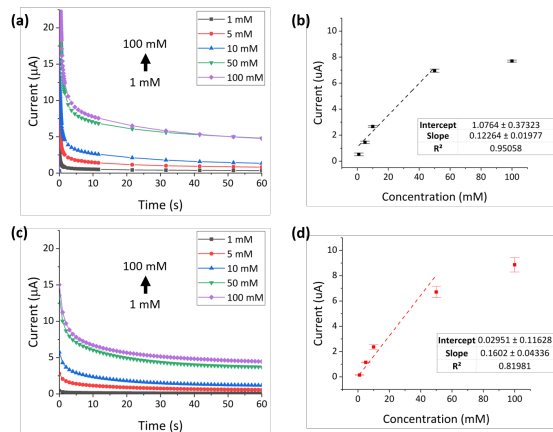


Fig. 6. Average CA response of glucose concentrations from 1 mM to 100 mM at a bias of +0.5V ($n=3$) and corresponding glucose calibration curves for (a,b) the benchtop potentiostat and (c,d) the solar-powered electrochemical system with linear regression shown from 1 mM to 50 mM.

CA validation of the amperometric system was conducted on both the benchtop potentiostat and solar-powered electrochemical systems ($n=3$) (Fig. 6) using commercial glucose test strips in solutions with glucose concentrations from 1 mM to 100 mM. The benchtop potentiostat with the test strips had a sensitivity of $0.123 \mu\text{A}/\text{mM}$ and showed a linear response with increasing glucose concentration in the 1 mM to 50 mM range ($R^2 = 0.951$). The solar-powered electrochemical system with the test strips had a sensitivity of $0.16 \mu\text{A}/\text{mM}$ and linear response with increasing glucose concentration in the 1 mM to 50 mM range ($R^2 = 0.82$).

The solar-powered electrochemical system was able to measure the OCP of the pH electrodes in various pH buffer solutions (Fig. 7). The potentiometric channel of the system measured a linear decrease in voltage with increasing pH ($R^2 = 0.992$), and the sensitivity of the solar-powered electrochemical system was $-0.053 \text{ mV}/\text{pH}$. Low-pass filtering and increased EMI shielding could further reduce the potentiometric noise.

IV. CONCLUSION AND FUTURE WORK

We present a solar powered wireless wearable metabolic sensing system with the capabilities of continuous amperometry and potentiometry, motion and temperature sensing, and light energy harvesting. *In-vitro* experiments were performed to characterize the energy harvesting capabilities of the system and validate the CV and CA capabilities of the system. The future efforts will focus on improving the system sensitivity and integration with custom electrochemical sensors, followed by short and long term *in-vivo* biochemical monitoring studies. Future improvements to this system also include transition to fully flexible electronics and replacement of the LiPo battery with a supercapacitor for faster charging and safer operation.

ACKNOWLEDGMENTS

The authors would like to thank Barbara Neal, Halston Deal, Dr. James Dieffenderfer, and Dr. Michael Lim.

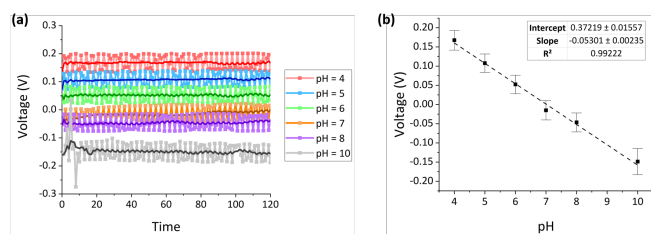


Fig. 7. (a) Potentiometric OCP measurement with overlaid 10 s MA filter output and (b) calibration curve for the solar-powered electrochemical system and a commercial pH electrode in pH = 4 to pH = 10 buffer solutions.

REFERENCES

- X. Li et al., "Digital Health: Tracking Physiomes and Activity Using Wearable Biosensors Reveals Useful Health-Related Information," *PLoS Biol.*, vol. 15, no. 1, pp. 1–30, 2017.
- J. Dieffenderfer et al., "Low-Power Wearable Systems for Continuous Monitoring of Environment and Health for Chronic Respiratory Disease," *IEEE Journal of Biomedical and Health Informatics*, vol. 20, no. 5, pp. 1251–1264, Sept. 2016.
- W. K. Lim et al., "Beyond fitness tracking: The use of consumer-grade wearable data from normal volunteers in cardiovascular and lipidomics research," *PLoS Biol.*, vol. 16, no. 2, pp. 1–18, 2018.
- B. Phypers and J. M. T. Pierce, "Lactate physiology in health and disease," *Contin. Educ. Anaesthesia, Crit. Care Pain*, vol. 6, no. 3, pp. 128–132, 2006.
- J. Finsterer, "Biomarkers of peripheral muscle fatigue during exercise," *BMC Musculoskelet. Disord.*, vol. 13, pp. 1–13, 2012.
- D. R. Seshadri et al., "Wearable sensors for monitoring the physiological and biochemical profile of the athlete," *npj Digit. Med.*, vol. 2, no. 1, p. 72, 2019.
- M. A. Yokus et al., "Wearable multiplexed biosensor system toward continuous monitoring of metabolites," *Biosens. Bioelectron.*, 2020.
- I. Ramfos et al., "A compact hybrid-multiplexed potentiostat for real-time electrochemical biosensing applications," *Biosens. Bioelectron.*, vol. 47, pp. 482–489, 2013.
- A. J. Bandodkar et al., "Tattoo-based noninvasive glucose monitoring: A proof-of-concept study," *Anal. Chem.*, vol. 87, no. 1, 2015.
- L. J. Curran et al., "Wearable Sensor System for Detection of Lactate in Sweat," *Sci. Rep.*, vol. 8, no. 1, pp. 1–12, 2018.
- W. Gao et al., "Fully integrated wearable sensor arrays for multiplexed in situ perspiration analysis," *Nature*, vol. 529, no. 7587, Jan. 2016.
- J. Dieffenderfer et al., "Towards a sweat-based wireless and wearable electrochemical sensor," *Proc. IEEE Sensors*, pp. 5–7, 2017.
- S. Imani et al., "A wearable chemical-electrophysiological hybrid biosensing system for real-time health and fitness monitoring," *Nat. Commun.*, vol. 7, no. May, pp. 1–7, 2016.
- G. Cappon et al., "Wearable continuous glucose monitoring sensors: A revolution in diabetes treatment," *Electron.*, vol. 6, no. 3, 2017.
- P. C. Shih et al., "Use and Adoption Challenges of Wearable Activity Trackers," *iConference Proc.*, no. 1, pp. 1–12, 2015.
- J. Zhao et al., "A Fully Integrated and Self-Powered Smartwatch for Continuous Sweat Glucose Monitoring," *ACS Sensors*, 2019.
- Y. Mao et al., "A self-powered biosensor for monitoring maximal lactate steady state in sport training," *Biosensors*, vol. 10, no. 7, 2020.
- H. Guan et al., "A self-powered wearable sweat evaporation biosensing analyzer for building sports big data," *Nano Energy*, vol. 59, no. February, pp. 754–761, 2019.
- I. Jeeran et al., "Wearable Skin-Worn Enzyme-Based Electrochemical Devices: Biosensing, Energy Harvesting, and Self-Powered Sensing," *Intech*, vol. i, p. 13, 2016.
- W. Han et al., "A Self-Powered Wearable Noninvasive Electronic-Skin for Perspiration Analysis Based on Piezo-Biosensing Unit Matrix of Enzyme/ZnO Nanoarrays," *ACS Appl. Mater. Interfaces*, vol. 9, no. 35, pp. 29526–29537, 2017.
- A. J. Bandodkar et al., "Sweat-activated biocompatible batteries for epidermal electronic and microfluidic systems," *Nat. Electron.*, vol. 3, no. 9, pp. 554–562, 2020.